A simple method to characterize the afterpulsing effect in single photon avalanche photodiode

H. T. Yen, S. D. Lin, and C. M. Tsai

Citation: Journal of Applied Physics **104**, 054504 (2008); doi: 10.1063/1.2968434
View online: http://dx.doi.org/10.1063/1.2968434
View Table of Contents: http://scitation.aip.org/content/aip/journal/jap/104/5?ver=pdfcov
Published by the AIP Publishing

A simple method to characterize the afterpulsing effect in single photon avalanche photodiode

H. T. Yen, S. D. Lin,[a] and C. M. Tsai
Department of Electronic Engineering, National Chiao Tung University, 1001 Ta Hsueh Road, Hsinchu 300, Taiwan

(Received 17 January 2008; accepted 13 June 2008; published online 3 September 2008)

A simple method is introduced for studying the afterpulsing effect in InGaAs single photon avalanche photodiode. The afterpulsing probability is obtained through measuring the detection efficiencies of various biasing pulses, while the incident photons are kept constant. The effect of excess bias and temperature on the afterpulsing probability is investigated. When the device temperature is higher than 170 K, the afterpulsing probability is lower than 5% for all excess bias voltages because the trapped carrier lifetime is much shorter than the repetition period. © *2008 American Institute of Physics*. [DOI: 10.1063/1.2968434]

I. INTRODUCTION

Single photon detectors are widely applied to ultralow power light detection and ultrafast optical measurement. The performance of single photon detection has made significant progress recently as a result of the growing demands in quantum cryptography, time resolved photoluminescence, and astronomical photometry.[1,2] Early single photon detection systems utilized photomultiplier tubes (PMTs) to detect single photons. The PMT has been gradually replaced by single photon avalanche photodiodes (SPADs) for single photon detection lately due to their high bias operation and low detection efficiency. Currently, the silicon (Si) SPAD has high detection efficiency (~70%), low dark count probability, and extremely weak afterpulsing effect at room temperature so it has been used for detecting single photons with wavelength below 1 μm. Meanwhile, the InGaAs SPAD attracts increasing attention owing to its ability of detecting single photons within the range of 1.3–1.55 μm, which is essential for a fiber-based long-distance quantum communication. However, the applications of InGaAs SPAD are limited by its serious afterpulsing effect.[3–6]

When an avalanche photodiode (APD) is operating in the Geiger mode, in which the bias across the APD is above its breakdown voltage, the electric field in avalanche region is so high that the breakdown current can be triggered by a single carrier. The amount of triggered output current depends on the excess voltage rather than on the incident photon numbers. Therefore, the power level of incident light is obtained with SPAD through counting of breakdowns. In order to have the SPAD breakdown sequentially for repetitive photon counting, the SPAD has to be shutdown after the breakdown is triggered and then it has to be restored for the next photon detection. At present, there are three methods of turning a SPAD off: passive quenching,[7] active quenching,[8,9] and operating in gated mode.[4] In passive quenching, one serially connects the SPAD with a large resistor that dismembers the voltage drop when the macroscopic (about tenths of microamperes) breakdown current is triggered thus the SPAD turns off automatically afterward. The active quenching implements an active circuit to lower the bias below the breakdown voltage for a short period of time after the trigger event. In the operation of gated mode, a pulsed voltage source is supplied to the SPAD to keep its bias above the breakdown voltage for a very short period of time and hence the SPAD can be triggered by a single carrier. That is particularly useful for the detection of repetitive single photons because one can minimize the detection period to suppress the dark count as well as to maintain the detection efficiency through synchronizing the incoming photons. Hence, the gated mode is widely used in the quantum communication.

To characterize the afterpulsing effect of InGaAs SPAD in the gated mode, one usually uses a time-delay method.[4] This method is complicated with its setup and not compatible with the conventional measurement of the SPAD's performance, such as dark count probability and detection efficiency. This makes it difficult to optimize the performance and, at the same time, to minimize the afterpulsing counts. In this report, we propose and demonstrate a method, which is easy to operate and is compatible with the performance characterization, to study the afterpulsing effect in the InGaAs SPAD.

II. EXPERIMENT RESULTS AND DISCUSSION

A. Measurement setup

In this work, an InGaAs APD manufactured by NEC (Product No. NR8300) is used. The setup system consists of three units (the biasing, signal processing, and light source units) and one device test chamber, as shown in Fig. 1. The biasing unit supplies the bias voltage to operate the APD in the gated mode. The unit is composed of a dc bias source (Keithley 230) and a pulse generator (HP 8114A). The signal processing unit, which includes a discriminator, a voltage amplifier, and a counter, processes the output signal of the APD. The discriminator and the amplifier are combined in a photocounting module and the counter comes from the Stanford Research System (SR400). In the light source unit, a

[a]Author to whom correspondence should be addressed. Electronic mail: sdlin@mail.nctu.edu.tw.Tel.: +886–3-5131240. FAX: +886-3-5724361.

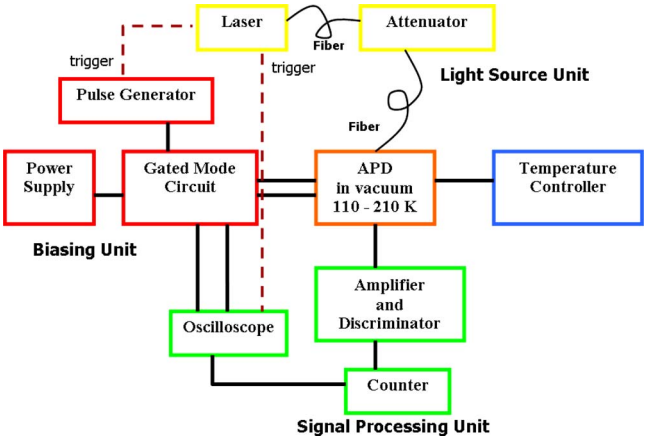

FIG. 1. (Color online) The system setup for single photon detection.

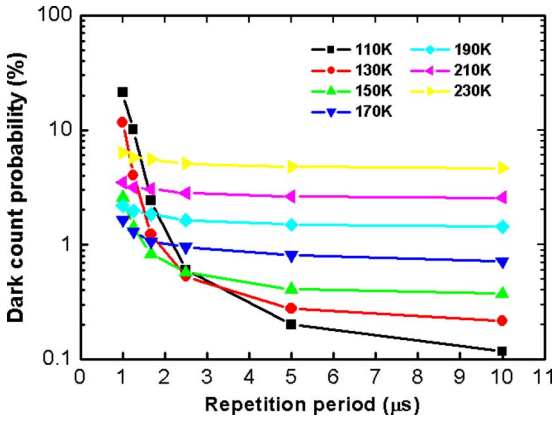

FIG. 3. (Color online) Measured dark count probabilities at 40 ns detection width with various repetition periods and temperatures.

1.3 μm pulsed laser (pulse width ~25 ps) with tunable repetition period is used. To avoid emitting two photons in one pulse, we set the output power at the level of 0.1 photon/pulse. The output power is measured by a power meter at a few nanowatts and then lowered down to 0.1 photon/pulse in average ($\sim 10^{-13}$ W) by a calibrated attenuator. The APD under test is cooled with liquid nitrogen and its temperature is controlled by a heating resistor. In order to synchronize the incident photons and the detection period, we connect the biasing and the light source units with a triggering signal and use a delay generator to compensate the delay time.

Typical measured waveforms are shown in Fig. 2. The bias voltage across the APD is, most of time, about 2 V below the breakdown voltage but goes over the breakdown voltage about 2.5 V (excess voltage) in a very short period of about 40 ns in which the APD can be triggered by single carriers in its avalanche region. As the current output waveform shown in Fig. 2, the SPAD is not triggered in each period even when the bias voltage is higher than its breakdown voltage. It clearly demonstrates the bistable current-voltage characteristic of the SPAD.[1] On the other hand, because the output current is not turned off before the end, the times of breakdown cannot be larger than one in each period. Accordingly, we calculate the triggered events by counting the number of periods in which the breakdown happens.

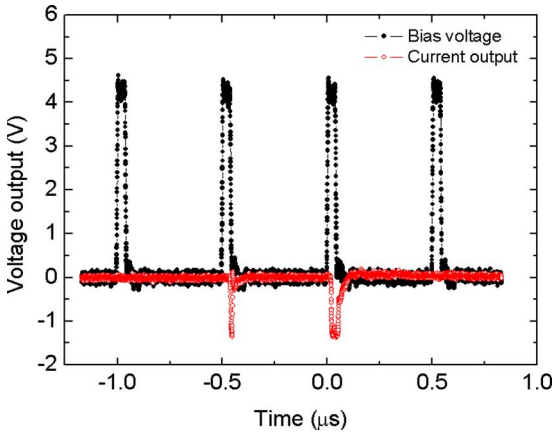

FIG. 2. (Color online) Measured waveforms of the bias voltage and the output current of a SPAD.

B. Results and discussions

The dark counts in a SPAD have two major origins: thermal and trap-released carriers. Thermal carriers caused by thermal excitation can trigger breakdown without any incoming photons and hence make wrong counts. These carriers can be largely suppressed by cooling down the SPAD. The trap-released carriers come from the previous breakdown events. When the breakdown happens, enormous carriers are generated and then the trapping centers are filled. The trapped carriers are released after a period of time (trapped carrier lifetime). If the trapped carrier lifetime is comparable to or larger than the repetition period, the released carriers may trigger breakdown events during the subsequent detection periods so that the dark count rate will increase and/or the photon count will be overestimated. This is known as afterpulsing effect. The afterpulsing effect can be eliminated by decreasing the repetition rate of detection. If the repetition period is much longer than the trapped carrier lifetime, the trapped carriers will be totally released in the off time of SPAD. However, longer repetition period means lower detection efficiency so that an optimization of the repetition rate is necessary to improve the performance of SPAD.

The dark count probabilities at each repetition period were measured at various temperatures, as shown in Fig. 3. At the repetition period of 10 μs, the dark count probability increases as the temperature increases because the higher temperature excites more dark carriers. However, as the repetition period becomes shorter, the dark count probability at 110 K grows dramatically. It is even higher than that at 230 K when the repetition period is 1 μs. This is reasonable if we consider the contribution of afterpulsing effect. The trapped carrier lifetime becomes longer as the temperature drops. At 110 K, the dark count contributed from the afterpulsing effect is negligible at the repetition period of 10 μs but it becomes dominant at 1 μs. The fact tells us that the trapped carrier lifetime is around a few microsecond. For a higher temperature, e.g., at 230 K, the trapped carrier lifetime becomes so short such that the measured dark count probabilities are nearly constant at all repetition periods.

As we have seen in the measurement of dark count probability, a lower temperature can suppress the dark count due to thermal carriers but, at the same time, it increases the

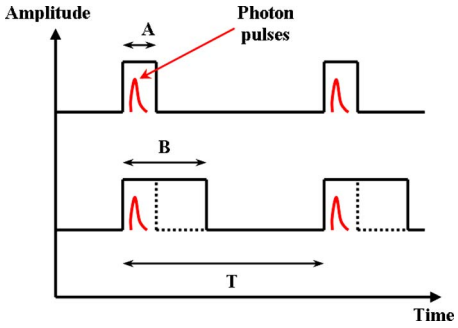

FIG. 4. (Color online) A schematic figure of our measurement method for analyzing the afterpulsing effect. Intervals *A* and *B* have different detection widths and the photons are synchronized and kept in the common interval *A*.

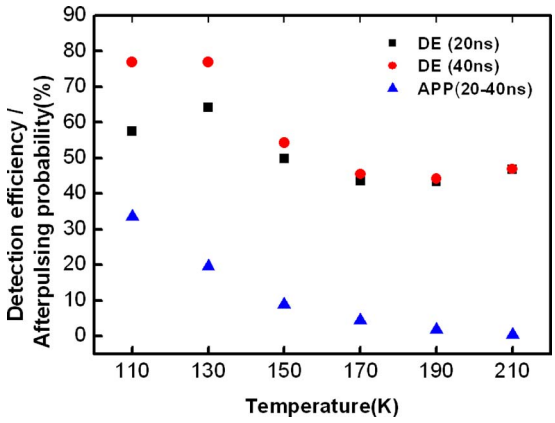

FIG. 5. (Color online) Measured detection efficiencies at 20 and 40 ns detection widths and the calculated afterpulsing probabilities.

afterpulsing counts from trapped carriers. In order to optimize the performance of SPAD, we introduce a quantitative method to characterize the afterpulsing effect under various conditions. The afterpulsing effect is governed by Eq. (1) below.[5] The average released carriers (N_r) within the duration time of detection width (Δt) is proportional to the average trapped carrier (N_{trap}) in one breakdown and to the dark count probability (P_d). It also largely depends on the repetition period (T) and trapped carrier lifetime (τ). Unsurprisingly, a longer repetition period or shorter detection width gives less released carriers as well as weaker afterpulsing effect, according to Eq. (1), which is as follows:

$$N_r = P_d N_{\text{trap}} \frac{\exp\left(\frac{\Delta t}{\tau}\right) - 1}{\exp\left(\frac{T}{\tau}\right) - 1}. \tag{1}$$

In conventional measurements, the afterpulsing probability is defined as the probability of a breakdown that triggers another breakdown afterwards in a detection width Δt and a repetition period T. According to Eq. (1), we can vary either the repetition period T or the detection width Δt to extract the afterpulsing probability because the P_d, N_{trap}, and τ are usually constant at a fixed temperature. In our method, with the consideration of simplicity, we fixed the T and analyzed the afterpulsing probability at various Δt. Figure 4 schematically shows our measurement method. At a fixed temperature, excess bias, and repetition period, the detection efficiencies of two detection widths (intervals *A* and *B*) were obtained with a constant incoming photon number in interval *A*. We can ensure that there is no additional photon coming into interval *B* by synchronizing the incoming photons with the detection pulse. Therefore, there should have no additional events detected in interval *B* if there is no afterpulsing effect. By means of calculating the differences of detection efficiencies between two intervals, we can establish the afterpulsing probability in the difference interval between intervals *A* and *B*. The validity of our method is revealed in the following equations:

$$\text{DE}_A = \frac{C_{\text{signal}}}{N_{\text{ph}}} \quad \text{DE}_B = \frac{C_{\text{signal}} \times (1 + \text{APP}_{B-A})}{N_{\text{ph}}}, \tag{2}$$

$$\text{APP}_{B-A} = \frac{(\text{DE}_B - \text{DE}_A) \times N_{\text{ph}}}{C_{\text{signal}}} = \frac{\text{DE}_B - \text{DE}_A}{\text{DE}_A}. \tag{3}$$

The notations are as follows: $\text{DE}_A(\text{DE}_B)$–the detection efficiency measured with interval *A* (*B*); C_{signal}—the signal count measured with interval *A*, N_{ph}—the number of incident photons in interval *A*, and APP_{B-A}—the afterpulsing probability in the difference interval between intervals *A* and *B*. If the power of incident light in interval *A* (N_{ph}) and the excess bias are fixed, the numbers of breakdown triggered by incoming photons will keep constant in different detection widths. In other words, the C_{signal} will be the same for the measurements of DE_A and DE_B. Accordingly, we can obtain the APP_{B-A} in Eq. (3) merely through measuring the DE_A and DE_B in Eq. (2). The afterpulsing probabilities in various conditions, e.g., temperatures, repetition periods, and excess bias, can be extracted and discussed in a quantitative way.

A typical measurement of the afterpulsing effect is shown in Fig. 5. The detection widths of intervals *A* and *B* were 20 and 40 ns. The repetition period was 10 μs and the excess bias was 3.5 V at all temperatures. The difference of detection efficiencies between 20 and 40 ns detection widths is significant at low temperatures (110–150 K) but approaches to zero at high temperatures (170–210 K). Using Eq. (3), the calculated afterpulsing effect is also plotted in Fig. 5. It is clear that the afterpulsing probability decreased as the temperature increased. This can be understood by noting that the trap carrier lifetimes are shorter at higher temperatures, so the afterpulsing effect is weakened at fixed repetition period, according to Eq. (1). The temperature dependence of afterpulsing is similar to reported literatures,[10–12] which confirm the validity of our scheme. However, a quantitative comparison is difficult as the afterpulsing effect is strongly dependent on the epitaxial structure, crystal quality, and device processing, so it varies from device to device.[11]

With the same method, we have also studied the influence of excess bias on the afterpulsing effect. The afterpulsing probabilities at 110, 150, and 190 K with a repetition period of 10 μs are shown in Fig. 6. We can see that, in the extreme case, the afterpulsing probability goes up to nearly 50% at 110 K with the excess bias of 4.5 V. Higher excess

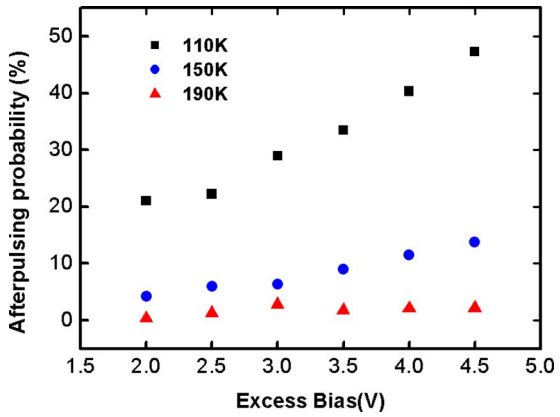

FIG. 6. (Color online) The afterpulsing probabilities obtained at various excess bias voltages at 110, 150, and 190 K.

bias enhances the afterpulsing effect because more carriers are generated and trapped. Furthermore, the afterpulsing probabilities at high temperatures are largely suppressed at all excess bias voltages, as the trapped carrier lifetime becomes much shorter than the repetition period at high temperatures. Based on the above, the optimization of the SPAD performance was achieved under the following conditions: $T=170-210$ K, repetition period $=10$ μs, and detection width $=20$ ns. The afterpulsing probability was lower than 5%, and the detection efficiency and the dark count probability were compromised to get the lowest noise equivalent power (NEP). As a result, the best performance of the InGaAs SPAD is 57% detection efficiency with a dark count probability of 1.2%, which has been obtained with 4.5 V excess bias and 20 ns detection width at 190 K. The calculated NEP is 7×10^{-16} $\mathrm{W/Hz^{1/2}}$.

III. CONCLUSION

We propose and demonstrate a simple method to characterize the afterpulsing effect in various conditions. The afterpulsing probability can be obtained through measuring the detection efficiencies at different detection widths provided that the synchronized incident photons are kept constant. We have found that the afterpulsing probabilities are less than 5% when the temperature is higher than 170 K. The best performance without the afterpulsing counts is 57% detection efficiency with 1.2% dark count probability. The corresponding NEP is 7×10^{-16} $\mathrm{W/Hz^{1/2}}$.

ACKNOWLEDGMENTS

This work was financially supported by the National Science Council of Taiwan under Contract Nos. NSC 96-2221-E-009-218 and 96-2120-M-009-010. The authors appreciate Dr. Pan in Truelight Inc. for his kind help with the device package. S.D.L. thanks P. L. Tang for her kind help.

[1] S. Cova, M. Ghioni, A. Lotito, I. Rech, and F. Zappa, J. Mod. Opt. **51**, 1267 (2004).
[2] M. Liu, X. Bai, C. Hu, X. Guo, J. C. Campbell, Z. Pan, and M. M. Tashima, IEEE Photonics Technol. Lett. **19**, 378 (2007).
[3] P. Hiskett, G. Buller, A. Loudon, J. Smith, I. Gontijo, A. Walker, P. Townsend, and M. Robertson, Appl. Opt. **39**, 6818 (2000).
[4] G. Ribordy, J. Gautier, H. Zbinden, and N. Gisin, Appl. Opt. **37**, 2272 (1998).
[5] Y. Kang, H. X. Lu, Y.-H. Lo, D. S. Bethune, and W. P. Risk, Appl. Phys. Lett. **83**, 2955 (2003).
[6] S. J. Fancey, G. S. Buller, J. S. Massa, A. C. Walker, C. J. McLean, A. McKee, A. C. Bryce, J. H. Marsh, and R. M. De La Rue, J. Appl. Phys. **79**, 9390 (1996).
[7] R. G. Brown, K. D. Ridley, and J. G. Rarity, Appl. Opt. **25**, 4122 (1986).
[8] R. G. Brown, R. Jones, J. G. Rarity, and K. D. Ridley, Appl. Opt. **26**, 2383 (1987).
[9] F. Zappa, M. Ghioni, S. Cova, C. Samori, and A. C. Giudice, IEEE Trans. Instrum. Meas. **49**, 1167 (2000).
[10] X. Jiang, M. A. Itzler, R. Ben-Michael, K. Slomkowski, M. A. Krainak, S. Wu, and X. Sun, IEEE J. Quantum Electron. **44**, 3 (2008).
[11] M. A. Itzler, R. Ben-Michael, C. F. Hsu, K. Slomkowski, A. Tosi, S. Cova, F. Zappa, and R. Ispasoiu, J. Mod. Opt. **54**, 283 (2007).
[12] K. E. Jensen, P. I. Hopman, E. K. Duerr, E. A. Dauler, J. P. Donnelly, S. H. Groves, L. J. Mahoney, K. A. McIntosh, K. M. Molvar, A. Napoleone, D. C. Oakley, S. Verghese, C. J. Vineis, and R. D. Younger, Appl. Phys. Lett. **88**, 133503 (2006).